

Covert Message Passing over Public Internet Platforms Using Model-Based Format-Transforming Encryption

Luke A. Bauer
University of Florida
lukedrebauer@ufl.edu

James K. Howes IV
University of Florida
james.howes@ufl.edu

Sam A. Markelon
University of Florida
smarkelon@ufl.edu

Vincent Bindschaedler
University of Florida
vbindsch@cise.ufl.edu

Thomas Shrimpton
University of Florida
teshrim@ufl.edu

Abstract

We introduce a new type of format-transforming encryption where the format of ciphertexts is implicitly encoded within a machine-learned generative model. Around this primitive, we build a system for covert messaging over large, public internet platforms (e.g., Twitter). Loosely, our system composes an authenticated encryption scheme, with a method for encoding random ciphertext bits into samples from the generative model’s family of seed-indexed token-distributions. By fixing a deployment scenario, we are forced to consider system-level and algorithmic solutions to real challenges — such as receiver-side parsing ambiguities, and the low information-carrying capacity of actual token-distributions — that were elided in prior work. We use GPT-2 as our generative model so that our system cryptographically transforms plaintext bit-strings into natural-language coverttexts suitable for posting to public platforms. We consider adversaries with full view of the internet platform’s content, whose goal is to surface posts that are using our system for covert messaging. We carry out a suite of experiments to provide heuristic evidence of security and to explore tradeoffs between operational efficiency and detectability.

1 Introduction

Format-Transforming Encryption (FTE) [9] is a symmetric-key encryption primitive that allows users to control the observable format of ciphertexts, by taking as input a specification of the allowed set of ciphertexts. Notably, changing the format of the ciphertext requires changing the format specification only. In this paper, we instantiate model-based FTE (MBFTE), a new kind of FTE scheme that uses machine-learned generative models to encode ciphertext formats. In particular, we build and analyze an MBFTE scheme whose ciphertexts mimic natural-language text. We use MBFTE as the core component of a covert message-passing system. Our main application of this system is "dead-drop" style covert communication, using large *public* internet platforms as dead-drops.

Many of these — Twitter, Mastodon, Reddit, Stack Exchange, etc. — are dominated by human-generated text, which makes the use of generative models a natural idea. The state-of-the-art in generative models for natural language has advanced considerably during the last 5 years, leading to a variety of text documents and news articles (e.g., one about the discovery of a new unicorn-like creature [25]) that are well-written and sometimes look realistic to humans.

In one case, a model-generated blog received over 26 thousand visitors until someone finally noticed that its articles were machine generated [27]. The MBFTE scheme that we build uses the Generative Pre-trained Transformer 2 (GPT-2), although the MBFTE architecture is not specific to this model. GPT-2 is a language model and generator that can be customized for specific textual domains and is open source.

Each dead-drop platform possesses its own unique quirks: the length of posts they admit, the categorization and threading techniques they rely upon (e.g., hashtags, handle/user pointers), slang and idioms, formatting conventions, etc. The system that we build around MBFTE must contend with these quirks. We note that by using large, public platforms, we do not rely upon cooperation or assistance from the dead-drop site; in fact, we want to use the platform in a way that even they do not notice.

At a high level, the sender-side processing flow is as follows. A plaintext string is encrypted using an encrypt-then-PRF [24] authenticated encryption scheme, and the resulting ciphertext is embellished with a relatively small number of additional bytes to form a ciphertext record. The record is then encoded into tokens that are sampled from a sequence of distributions, presented by the generative model and dependent upon the current seed, by treating the ciphertext-record bits as a codeword and decompressing these via arithmetic decoding. On the receiver side, the sequence of received tokens is recompressed via arithmetic encoding (and the same sequence of model distributions) to recover the ciphertext record, and that is decrypted to recover the plaintext.

Challenges in practice. While this approach is conceptually

straightforward and has been applied in some prior work [6, 19, 20, 30, 32, 36], there is much to be done in order to address implementation and deployment realities that arise from using generative models, and co-opting large public platforms for covert-message passing. Prior work has largely elided these matters, and most of our system-building effort is aimed at tackling them head-on.

To begin, generative models for natural language such as GPT-2 [28] and BERT [7] use subword tokenization strategies, often derived from byte-pair encoding, for compression and as a way to deal with rare words. This means that generated text will be the concatenation of subword tokens; this poses no parsing problems for human readers (sensitivity of the text aside) but is a significant challenge in our setting. Namely, generated tokens encode one or more hidden bits. So when the receiver encounters (say) the word *these*, it must determine how to parse this: is the first token *t*, *th*, *the* or *these*? All of these may be valid tokens in the current token distribution. Succinctly, the strings that are produced by encoding bits into sequential samples from the support of GPT-2s generative distributions are not uniquely parseable. Our system’s receiver side processing must deal with this ambiguity, and there are important time/memory efficiency vs. correctness tradeoffs to be balanced. This is an important challenge that seems not to have been addressed by prior works (e.g., [6, 32, 36]) that use generative models for steganographic/covert messaging.

Additionally, the number of hidden bits that one can encode within each sampled token depends crucially on the min-entropy (in particular) of the token distribution presented by the model. For "realistic" text, these distributions admit less than 10 bits of capacity per sample; even less, on average. In theory, this is not a problem: one simply allows the covert-text to be as long as it needs. But very long coverttexts may be suspicious on platforms where these are uncommon, and many platforms may impose length limits. To deal with this, our system supports fragmenting the plaintext across multiple coverttexts.

When Alice sends messages to Bob, via one or more covert-texts written to the dead-drop platform, Bob faces the non-trivial task of determining *which* platform messages to retrieve. Of course, he could simply retrieve all messages (written, say, within a given time window) and try to recover from them a message from Alice. This naive approach is unlikely to scale for real platforms that host millions of users and many millions of posts each day. So, Bob needs a "hint" as to which messages he should retrieve. As the platform should remain unaware of its use as the dead-drop, it cannot be relied upon to help. Thus, Alice’s coverttexts must hint *at themselves*, but only to Bob. Our system uses a combination of overt coverttext hints (e.g., ensuring that the coverttexts contain a particular hashtag) and hidden cryptographic hints that allow Bob to process only a few tokens of a candidate coverttext and reliably determine whether or not this message was created by our MBFTE system with the correct key. Note the obvious trade-

offs here: if the overt hint is too unique, then it may provide an accurate distinguishing marker for an adversary; if it is too common, then Bob must scrape and perform at least some amount of processing on a prohibitive number of platform messages that are not meant for him.

Adversarial model and Experimental Findings. We consider an adversary with a potentially global view of all posts to the platform, and with the knowledge that some users may be employing our system to exchange covert messages. The adversarial goal is to identify posts that contain MBFTE messages or to establish if a (suspected) individual is indeed communicating over the platform using MBFTE messages.

Even with state-of-the-art language models, we expect that a determined human examiner could distinguish MBFTE coverttexts from genuine platform posts. But for a large public platform, like Twitter, that receives over 500 million tweets per day (6000 tweets per second), scaling this approach would require extreme measures. As such, we focus on automated strategies to distinguish MBFTE messages from other, normal platform messages.

Following all previous work in this space [6, 10, 23, 35, 36], we do not provide a provable-security analysis of our system; there is no formal definition of security for systems like ours, in our envisioned deployment scenario. We explore security via a suite of principled experimental results. Specifically, we pit our system against three types of adversaries that we model as machine learning algorithms, including one that uses OpenAI’s state-of-the-art detector for GPT-2. Our experiments explore the effects of *a priori* knowledge on adversarial success, e.g., whether or not the adversary precisely knows the GPT-2 parameters or initial coverttext seed that we use.

We find that fine-tuning the model and setting appropriate seeds for each message ensures that the produced coverttexts resemble messages posted on the platform, which makes identifying MBFTE more challenging for adversaries.

In addition, even our strongest adversary — one based on a state-of-the-art detector *against GPT-2* (RoBERTa), and given full knowledge of the specific fine-tuning used — cannot identify MBFTE messages without also flagging a large number of normal platform messages as suspect, i.e., incurring a large false-positive rate. The reason for this is that, on a large public platform, the proportion of MBFTE messages on the platform will be much less than 1% of the overall number of messages posted. Whenever this base rate of MBFTE messages is smaller than the adversary’s false-positive rate, we find that the overwhelming majority of flagged messages are false alarms.

Taking Twitter as an example, if the false positive rate is 0.1% (the lowest we have observed experimentally for our strongest adversary) over 500,000 tweets per day will be flagged as MBFTE. Of these, only 2.19% would be actual MBFTE messages if the base rate is 0.01%, which would still allow for over 50,000 covert messages to be exchanged

per day. Further, the majority (77.6%) of MBFTE messages would remain undetected (i.e., not flagged).

Our experiments also shed light on the tension between system efficiency (in terms of computation and message-carrying capacity) and security. An example of this tension is the tuning of the temperature parameter of the model, which controls the shape of the token distribution. Using a large value for the temperature allows more bits to be embedded in each sampled token, hence better goodput. However, this also decreases the naturalness of coverttexts, which makes it easier for adversaries to identify MBFTE messages. Therefore, we allow for temperature and other parameters to be set by the user to fit their specific requirements. For instance, a user who is less concerned with security and more concerned with capacity could set a larger temperature.

As a final note, our system also provides mechanisms to protect against adversaries that may actively alter posts. It is unclear how realistic this threat would be for large, public platforms—particularly when the adversary’s goal is to identify suspicious posts across the platform, as opposed to looking for evidence of covert messaging by a specific user of the platform—but such threats were in mind as we designed our system.

2 Background and Related Work

Formatted encryption. The core intuition behind formatted encryption is straightforward: since practical encryption primitives (i.e. block ciphers) are idealized as pseudorandom permutations (PRP) over integer domains, any language for which there exists an efficiently computable bijection to non-negative integers can be used as a plaintext or ciphertext *format* for a formatted encryption scheme. It was first instantiated by the format-preserving scheme of Bellare et al. [4] which accepts a DFA-specified regular language as both plaintext and ciphertext format.

Dyer et al. [9] created the first format-transforming scheme in their work on evading Internet censorship, using regular expressions extracted from censorship DPI boxes as output formats, which were subsequently included in the Tor [8] browser bundle as a “pluggable transport” traffic-obfuscation method. Follow-on work by Luchaup et al. [21] developed a new FTE method that worked from more space-efficient NFA representations. This method also supports FTE from context-free grammars (CFG), thereby allowing syntactically correct C-language source code (among other things) to be used as the ciphertext format [22].

Neither regular expressions nor CFGs provides good models of natural language text, so no previous realization of FTE is appropriate for our target application. Both NFA- and CFG-based formatted encryption required clever algorithms to handle the inherent ambiguity of the language representations and avoid computationally intractable schemes. With

model-based FTE we encounter a similar issue with ambiguity, and it is instructive to compare the techniques of prior FPE/FTE constructions with the approach we present in Section 3.

Model-based steganography. We present MBFTE as an extension of formatted encryption, but it shares a common structure with many proposals appearing in the literature on steganography. Steganography is an information-hiding technique that seeks to conceal the *presence* of a message within a communication medium. The typical threat model for steganographic communication can be attributed to Simmons’ *prisoners’ problem* [33], and most of the key research problems were identified in an early survey by Anderson and Petitcolas [2].

Although the central idea was not unique to his work, Sallee coined the phrase *model-based steganography* [30] to describe a system in which a model of the cover medium provides a conditional probability distribution that is used to embed an encrypted message through source coding. Similar schemes based on source coding have also been proposed for the complexity-theoretic setting, in which the distribution over cover messages is learned through stateful black-box sampling [19] or by modeling the channel as an efficiently learnable concept class [20].

Natural language steganography. A number of recent papers have explored the use of natural language models generally and GPT-2 specifically in generating steganographic text using techniques similar to model-based steganography. Yang et al. [35] combined a recurrent neural network (RNN) model with Huffman coding, and Dai and Cai [6] provided a less detectable Huffman coding algorithm with GPT-2 as the language model. Ziegler et al. [36] applied arithmetic coding to GPT-2 and demonstrated that it consistently outperforms Huffman coding, and Shen et al. [32] improved upon their results by dynamically adjusting the depth of the model distribution with each token (a technique also known as *nucleus sampling* [15]). In a paper concurrent with this work, Kaptchuk et al. [17] describe a novel coding technique called *Meteor* which yields a modest improvement in the KL-divergence of the model output compared to arithmetic coding, although this comes at the cost of a 50% increase in coverttext length.

While we use the same fundamental techniques, we have made explicit—and devised solutions for—a number of challenging implementation details that are not addressed in this prior work.

Dead-drop covert messaging. Our covert messaging system architecture can be compared most closely with Collage, a framework for developing censorship-resistant applications through user-generated content posted on public Internet platforms [5]. The authors describe this as “deniable asynchronous point-to-point communication”, commonly referred to as *dead-drop* communication. The Collage framework establishes a layered architecture for covert network

applications, with a *message layer* that provides semi-reliable delivery and a *vector layer* that provides covert transport capacity. In this model, our messaging system could be viewed as an implementation of a vector layer transport.

An important issue identified by Collage is the need for efficient filtering of covert messages from among the large volume of content on public platforms. They implicitly accomplish this through a technique we call *semantic signaling* in which an overt semantic attribute of the content enables the receiver to filter potential covert messages. This concept is relevant to our system implementation in Section 4.

3 Model-based FTE

In this section, we provide a technical definition of model-based FTE, the core of our covert messaging system, and then detail a particular construction of an MBFTE scheme. First, let us establish some notation that will be used throughout the remainder of the paper.

Notational preliminaries. When X, n are integers, we write $\langle X \rangle_n$ to denote the n -bit string that encodes X . When a, b, c are integers, we write $\llbracket a \rrbracket_c^b$ and $\llbracket a \rrbracket_c^b$ as shorthand for $(a \cdot 2^c) \% 2^b$ and $\lfloor (a \% 2^b) \cdot 2^{-c} \rfloor$, respectively (we call them *bounded bit shifts*). When X, Y are strings, we write $X \parallel Y$ for their concatenation and $|X|, |Y|$ for their lengths. We write $X[i]$ for the i th symbol in X , $Y[-i]$ for the i th-to-last symbol in Y , and $X[:i]$ for the string consisting of the first i symbols in X .

We use standard pseudocode to describe algorithms, with a few expressive embellishments: When \star is a binary operator, the statement $a \leftarrow \star b$ is equivalent to $a \leftarrow a \star b$. We use the statement $a \leftarrow \lambda x. \Phi$ in a similar manner, evaluating expression Φ with a in place of each x , and assigning the result to a . If multiple comma-separated variables appear on the left side of such an assignment, then the operation is applied to each in turn. The expression $\$(n)$ uniformly samples an integer between 0 and $n - 1$.

Model-based formats and FTE schemes. A *model-based format* is a tuple $\mathcal{M} = (\Sigma, \mathcal{S}, \mathcal{F}, \text{Next}, s_0)$ where Σ is a set of *tokens*, \mathcal{S} is a set of *model seeds*, $\mathcal{F} = \{f_s\}_{s \in \mathcal{S}}$ is an ensemble of distributions over values in Σ , $\text{Next} : \mathcal{S} \times \Sigma \rightarrow \mathcal{S}$ defines a *seed transition function*, and $s_0 \in \mathcal{S}$ is the initial seed. A *model-based FTE scheme* (MBFTE) is a pair of algorithms (Enc, Dec) with the following specification:

- The deterministic encryption algorithm (Enc) takes as inputs a key K , an initial value N , a model-based format \mathcal{M} , and a plaintext string M ; it outputs a ciphertext string $X \in \Sigma^*$. We write $X \leftarrow \text{Enc}_K^{N, \mathcal{M}}(M)$.
- The deterministic decryption algorithm (Dec) takes as inputs a key K , an initial value N , a model-based format \mathcal{M} , and a ciphertext string X ; it outputs a plaintext string M or the distinguished error symbol \perp . We write $M \leftarrow \text{Dec}_K^{N, \mathcal{M}}(X)$.

An MBFTE scheme is δ -*correct* if for all N, \mathcal{M} , and M we have $\Pr[\text{Dec}_K^{N, \mathcal{M}}(\text{Enc}_K^{N, \mathcal{M}}(M)) = M] \geq \delta$ with probability taken over the choice of K ; for sufficiently small values of δ we may simply refer to the scheme as *correct*. These two definitions support formatted encryption schemes for a particular class of generative model; specifically, those which can deterministically produce a family of arbitrarily long distribution sequences from a starting seed.

Sampling as source decoding. To transform a plaintext string into a formatted ciphertext, we utilize the same technique as previous work on model-based steganography: encrypt the string, interpret this ciphertext as a source code for the distribution provided by the model, and “decompress” it using standard source-coding algorithms. This procedure is more nuanced than it may appear because source-coding algorithms are designed in the *forward* direction—given an input string, an optimal encoding for that string will uniquely decode to the same string—but model-based FTE applies these algorithms in the reverse order.

The key challenge is that the ciphertext may not line up with any particular discrete source code implied by the model distribution(s), resulting in ambiguity at the end of the coding process. For example, one can sample a token from a Huffman tree by using the ciphertext bits to choose branches until a leaf is reached, but this process may run out of bits before fully traversing the tree on the final token. A similar problem occurs in arithmetic coding, where the remaining ciphertext bits may not have enough precision to unambiguously choose a final token.

In either case, there are two options to ensure that the decoder terminates: pad the ciphertext with extra bits until a unique token can be chosen, or ignore any partially decoded output (effectively truncating those bits). Both options introduce ambiguity when the resulting format string is encoded during decryption since the encoder does not know *a priori* how many bits were added to, or truncated from, the original ciphertext. If the ciphertext was produced by an authenticated encryption scheme then trial decryption can be used to resolve this ambiguity, as long as the expected number of trial decryptions required is small to avoid any substantial impact to security or efficiency.

MBFTE using arithmetic coding. As discussed in Section 2, efficient FTE schemes can be constructed from (relaxed) ranking schemes for certain classes of formal languages. In our MBFTE construction, an arithmetic coding scheme over the generative model takes the role of the ranking scheme in mapping the domain of the cipher to the domain of the format. We use a fixed-precision arithmetic coding algorithm similar to those described by Rubin [29] and Howard & Vitter [16]; refer to Figure 1 for a pseudocode description.

The system is parameterized by a symbol length r , which denotes the bit length of each symbol (e.g. $r = 8$ for byte strings) and coding length ℓ which determines the size of the

```

1 procedure Decode( $C, \mathcal{M}$ ):
2    $w, a, b, c \leftarrow 0, 0, 2^{r\ell}, C[:\ell]$ ;  $T, D \leftarrow \varepsilon$ ;  $s \leftarrow \mathcal{M}.s_0$ 
3   repeat
4      $t \leftarrow \text{GetToken}(\mathcal{M}.F_s, \frac{c-a}{b-a})$ ;  $T \leftarrow \|t$ 
5      $a, b \leftarrow \text{Adjust}(\mathcal{M}.F_s, t, a, b)$ 
6      $\text{Rescale}(D, w, a, b, c, C)$ 
7      $s \leftarrow \mathcal{M}.Next(s, t)$ 
8   until  $|D| \geq |C|$ 
9   return  $T$ 

10 procedure Encode( $T, \mathcal{M}$ ):
11    $w, a, b \leftarrow 0, 0, 2^{r\ell}$ ;  $D \leftarrow \varepsilon$ ;  $s \leftarrow \mathcal{M}.s_0$ 
12   for  $t$  in  $T$  do
13      $a, b \leftarrow \text{Adjust}(\mathcal{M}.F_s, t, a, b)$ 
14      $\text{Rescale}(D, w, a, b)$ 
15      $s \leftarrow \mathcal{M}.Next(s, t)$ 
16   return  $D, w$ 

17 procedure Adjust( $\mathcal{F}, t, a, b$ ):
18    $F, f \leftarrow \text{GetFreq}(\mathcal{F}, t)$ 
19    $a, b \leftarrow a + \lfloor (F + f) \cdot (b - a) \rfloor, a + \lfloor F \cdot (b - a) \rfloor$ 
20   return  $a, b$ 

21 procedure Rescale( $D, w, a, b, c, C$ ):
    // arguments passed by reference
    // shaded code is elided when  $c, C$  not passed
22   repeat
23     if  $w > 0$  and  $\lfloor a \rfloor_{r, \ell-1}^{r\ell} = \lfloor b \rfloor_{r, \ell-1}^{r\ell}$  then
24        $D[-w] \leftarrow \lfloor a \rfloor_{r, \ell-1}^{r\ell}$ 
25       for  $i \leftarrow 1..(w-1)$  do  $D[-i] \leftarrow \neg D[-i]$ 
26        $w \leftarrow 0$ ;  $a, b, c \leftarrow \oplus 2^{r\ell-1}$ 
27     if  $b - a < 2^{r \cdot (\ell-1)}$  then
28        $A \leftarrow \lfloor a \rfloor_{r, (\ell-1)}^{r\ell}$ ;  $D \leftarrow \|A$ 
29        $a, b \leftarrow \lambda x. \lfloor x \rfloor_r^{r\ell}$ 
30       if  $A \neq \lfloor b \rfloor_{r, (\ell-1)}^{r\ell}$  then
31          $a, b, c \leftarrow \oplus 2^{r\ell-1}$ 
32         if  $|D| + \ell \leq |C|$  then  $c \leftarrow C[|D| + \ell]$ 
33         else  $c \leftarrow \$(2^r)$ 
34          $w \leftarrow +1$ 
35   until  $b - a > 2^{r \cdot (\ell-1)}$ 

36 procedure GetToken( $\mathcal{F}, F$ ): Returns the first token  $t$ 
    from  $\mathcal{F}$  with cumulative frequency  $\geq F$ .

37 procedure GetFreq( $\mathcal{F}, t$ ): Returns the cumulative
    frequency  $F$  and relative frequency  $f$  of token  $t$  in
    distribution  $\mathcal{F}$ .

```

Figure 1: Fixed-precision arithmetic coding algorithms for use in MBFTE.

coding range in symbols. The precision of the coding state is therefore fixed at $r \cdot \ell$, with the lower bound in a and the upper bound in b . The core of both encoding and decoding is a loop which (1) adjusts the coding range based on the current token, (2) rescales the coding range to shift out determined symbols, and (3) updates the model seed. When rescaling, the range may need to be "inverted" if it straddles a symbol boundary; w keeps a count of symbols that were output in an inverted state, and lines 24–25 adjust these symbols when the inversion is resolved.

During decoding the next token is selected from the model distribution according to the ciphertext bits that are in the coding window (represented by c). As symbols are shifted out and appended to D , the remaining ciphertext symbols are shifted into the coding window one by one. Once the end of the ciphertext is reached, random padding bits are used to maintain a uniform sampling of tokens. The loop terminates once the full length of the ciphertext has been shifted out, at which point D should be equal to C , or at least within a small margin of error depending on the value of w and how many padding bits (if any) were shifted out on the final token.

Encoding proceeds in a similar manner, except that the sequence of tokens is provided as input rather than sampled from the model. This parallel operation ensures that, as long as the model \mathcal{M} is identical, the value of D returned by the encoder will be the same value produced by the decoder. We must also return w because the trailing w symbols will have two alternatives depending on how the inversion could resolve, so both must be considered.

Constructing an MBFTE scheme is now a straightforward composition of the arithmetic coding algorithms with a deterministic AE scheme $\Pi = (\mathcal{E}, \mathcal{D})$ (with keys $K \in \mathcal{K}$ and IVs $N \in \mathcal{N}$) as follows:

- $\text{Enc}_K^{N, \mathcal{M}}(M)$: Output the value returned by $\text{Decode}(\mathcal{E}_K^N(M), \mathcal{M})$.
- $\text{Dec}_K^{N, \mathcal{M}}(X)$: Compute $C, w \leftarrow \text{Encode}(X, \mathcal{M})$. Then,
 1. Compute $M \leftarrow \mathcal{D}_K^N(C)$. If $M \neq \perp$, output M and halt.
 2. If $w > 0$ then let $C' \leftarrow C$ and compute $C'[-w] \leftarrow +1$. If $w > 1$, invert the bits in the last $w - 1$ symbols of C' . Compute $M \leftarrow \mathcal{D}_K^N(C')$. If $M \neq \perp$, output M and halt.
 3. Subtract 1 from w , truncate the last symbol from C and return to (1), unless $\ell - 1$ symbols have already been truncated, in which case output \perp and halt.

The worst-case number of trial decryptions required is 2ℓ , although with suitable values of r and ℓ this number can be minimized in practice during honest operation. An active attacker that knows the model distribution can swap the randomness used for the padding, so we should assume that the worst-case will occur for an adversarially chosen forgery. Concretely, for parameters $r = 8, \ell = 4$ which we use in our empirical testing,

we would expect the adversary to succeed in creating a valid ciphertext forgery about 8 times as often as the upper bound assumed for the underlying AE scheme.

The ambiguity introduced by reversing the normal source coding algorithms is similar to the issues faced in prior FTE schemes. However, in those cases, it is possible to “pre-disambiguate” on the encryption side, by e.g. cycle-walking past non-invertible values [21]. Here, we must resort to a trial decryption strategy instead, which slightly weakens the security provided by the underlying AE scheme as well as the correctness guarantee of the composition.

In the next section, we describe our covert messaging system using MBFTE, which has a few further modifications to reduce the likelihood of these worst-case outcomes.

4 MBFTE-based Messaging System

In this section, we describe the sending and receiving processes of our covert messaging system. Along with platform-specific processing, our implementation uses the MBFTE scheme described in the previous section with some embellishments that allow us to (1) avoid the worst-case of 2ℓ trial decryptions, and (2) handle ambiguity when the coverted string does not have a unique parse into tokens.

Note that in this section we use the term *coverted* to refer to the formatted ciphertext output of the MBFTE scheme, to align with common steganographic terminology used in describing similar systems.

4.1 Ciphertext record construction

Our underlying AE scheme is a slightly modified encrypt-then-PRF generic composition [24] of CTR-mode and HMAC. The inputs are a plaintext message M , a message-independent initial value $IV \parallel IX$ that is the concatenation of a CTR-mode IV (IV) and a *coverted tweak* (IX), and key $K = (K_1, K_2, K_3)$. First, we transform the input message M into $M' = \langle |M| \rangle_t \parallel M$. Our implementation sets $t = 16$, but this is strictly an engineering choice and is adjustable. (If $|M| > 2^t$, assume the scheme immediately returns \perp .) We encrypt M' using CTR-mode with IV and K_3 to produce ciphertext C . In parallel, we generate a *sentinel value* (SV) by computing $\text{HMAC-SHA512}_{K_1}(\text{“SV”} \parallel IV \parallel IX)$ and truncating the result to a two-byte value V . (The purposes of the coverted tweak and sentinel value will be discussed in a moment.) Finally, we generate the authentication tag T by computing $\text{HMAC-SHA512}_{K_2}(\text{“Tag”} \parallel V \parallel C)$ and truncating the result to five bytes. The *ciphertext record* is the string $V \parallel C \parallel T$. Again, the choices of two bytes for the SV and five bytes for the tag are to balance security and efficiency, and are adjustable.

Strictly speaking, this is not a pure encrypt-then-PRF construction, because (1) the input M is transformed into $M' = \langle |M| \rangle_{16} \parallel M$, and (2) we transmit (and tag) $V \parallel C$ rather

than C alone. As the sentinel value V is independent of the message M , neither of these modifications affect security. In fact, it is straightforward to modify the standard security proof for encrypt-then-PRF (from CTR-mode and HMAC) to our construction. Moreover, our “transform-then-encrypt-then-sentinel-then-PRF” construction remains an AE scheme, as needed for the composition described in Section 3.

Note that the implementation just described does not transmit the initial value $IV \parallel IX$ as part of the ciphertext record. This is strictly for performance reasons: the ciphertext record will be decoded into a coverted via the token distribution(s) presented by the model, and we will see that each additional record bit can incur significant expansion of the coverted. The operational implication is that the receiver will need to rederive the correct IV and IX by other means (e.g., shared state or out-of-band communication). If this is not feasible in the deployment environment, and the IV must be transmitted in the ciphertext record, care should be taken to ensure that the entire ciphertext record remains pseudorandom (for proper sampling from the model) and that the tag covers the IV, too.

Finally, note that we do not apply any compression to the plaintext message M prior to encryption. Doing so could significantly improve capacity/throughput in cases where the plaintext is highly compressible but it could also make the system vulnerable to compression side-channel attacks [1, 13, 18].

4.2 Sender-side operation

The communicating parties must share secret keys K_1, K_2, K_3 , and generative model \mathcal{M} with initial seed s_0 . Whether the model and seed are secret has implications for our (upcoming) detectability tests, but it is not relevant to the operation of the system.

Step 1: Build the ciphertext record. To send a message M , the sender first chooses a coverted tweak IX from a fixed set of possible values, concatenates this to an appropriately chosen CTR-mode IV, and then computes a ciphertext record $W = V \parallel C \parallel T$ through the process just described. The set of coverted tweaks can (and typically should) be small, as we will see.

Step 2: Record bits \rightarrow Model tokens. The ciphertext record and model are provided as input to the arithmetic decoder described in Section 3. This decoding produces a sequence of model tokens, each drawn from a corresponding sequence of seed-dependent token distributions presented by the model. After each token is produced it is combined with the current seed to generate a new seed, which for many generative models (including GPT-2) is accomplished by simply concatenating the token to the seed. In this manner, the next model distribution implicitly depends on the tokens used to generate the coverted so far.

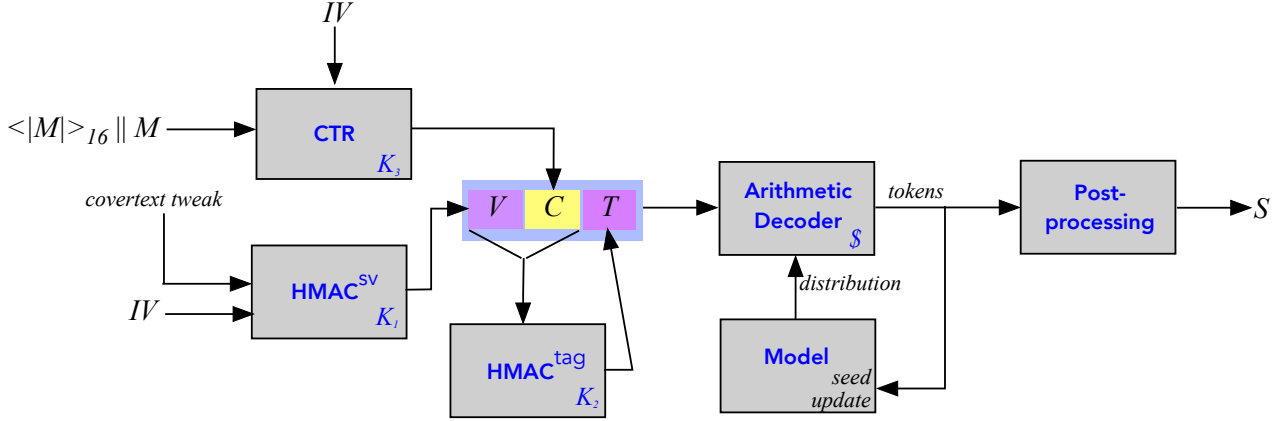


Figure 2: Sender-side flow.

Tweaking the model outputs. Here, the purpose of the covertext tweak IX becomes apparent: it influences the *initial randomness* used to start the decoding process. Since it is used in calculating the SV which is the first two bytes of the ciphertext record, it strongly influences the first few tokens selected from the model. These tokens, in turn, influence the distributions from which all subsequent tokens are chosen. The end result is that varying the covertext tweak allows one to produce a set of highly varied covertext outputs for the same message. In a deployment scenario that requires undetectability against human observers, this can be used to allow the sender to select the most natural-looking covertext from a group of options.

Step 3: Add (overt) semantic signals to the covertext.

The final step of sender-side operation (Fig. 2) is to post-process the sequence of tokens that comprises the covertext to add platform-specific semantic signals (e.g. hashtags for social media content) at well-defined locations. These signals are overt, in the sense that they are publicly visible, and do not depend on the cryptographic operations that created the covertext. The output of post-processing is the cover content S that is submitted to the dead drop platform for posting.

As we briefly discussed in the background on dead-drop messaging, semantic signaling is an important aspect of practical architectures because it reduces the burden of finding covert messages hidden among the potentially massive set of content on the platform. In general, good semantic signals must strike a balance between efficiency and undetectability, as they determine the amount of content that the receiver must sift through but may also reveal the presence of covert messages to an adversary. Therefore, in addition to this overt signal, we use the SV as a covert signal to improve receiver efficiency without harming detectability.

4.3 Receiver-side operation

After collecting a set of potentially covert content from the platform using the semantic signal, the receiver processes each piece of content in turn, extracting a covert message or discarding the content as soon as it determines that it does not contain a covert message. This process (Figure 3) can be efficiently pipelined so that the full sequence is only performed on those items that almost certainly do contain a covert message.

Parsing non-prefix-free token sets. We first pre-process the input string to remove extra formatting and semantic signals explicitly added by sender-side post-processing, giving us the base covertext. The MBFTE decryption algorithm operates on a tokenized string, but many generative models (especially natural language models) use token sets that are *not* prefix-free and thus the covertext may not be uniquely parseable. To handle this ambiguity we utilize a top- N parsing strategy, in which we maintain up to N most likely parse paths after each token. Intuitively, this can be visualized as growing a tree of possible parsings and trimming off all but the N most likely branches at each step.

For example, suppose the first word of the covertext is “These”, and the tokens ‘ T ’, ‘ Th ’, ‘ The ’, ‘ $These$ ’ appear in the support of the initial token distribution. If $N = 3$ then we would select the three most likely tokens from among these four and continue parsing each in parallel, updating the seed and generating a new token distribution for each. If any of these result in additional ambiguous parsings, we compare the joint probabilities and always maintain only the top N options at each step. Any branches which fail to parse (i.e. no token matches a prefix of the remaining covertext) are removed as well.

Checking sentinel values. Since the encoder examines only a single token for each iteration of the coding loop, we can effectively pipeline the parsing process into encoding and

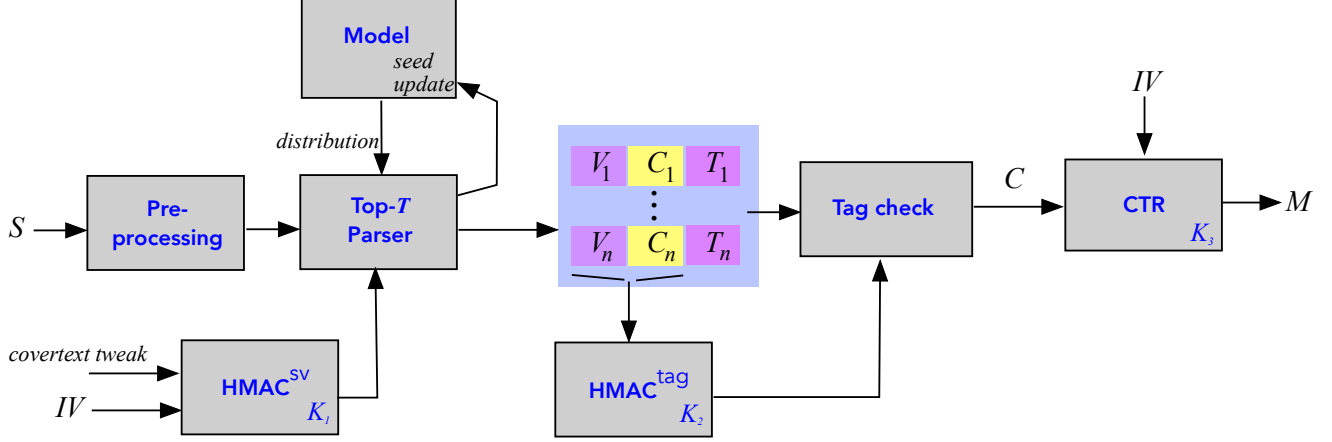


Figure 3: Receiver-side flow.

decryption, taking advantage of our ciphertext record structure to minimize wasted effort on incorrect parse paths. Each parse branch maintains a parallel encoding as well, and as tokens are added to the parse we can immediately encode them to grow the code output. Once sufficient tokens have been encoded to unambiguously determine the first two bytes of the code for a given branch, we can verify if these bytes constitute a valid SV. If so then we continue parsing along that path; otherwise, the path is eliminated from the set of N active paths. Since the receiver does not know which covertask tweak the sender chose, they do not know the exact value of the SV they are looking for. So whenever they check an SV, they brute force check it against the possible SV values, each associated with a tweak value. The tweak range is kept small, 1-10, so this has virtually no impact on decode time.

Blockwise decryption. Once a parse path is confirmed to encode a valid SV, we can begin pipelining the decryption process as well. Recall that the ciphertext record construction is $V||C||T$ where C is a CTR-mode encryption of the message M prepended with its length $\langle |M| \rangle_{16}$. This allows us to sequentially perform block-wise decryption on each additional block of encoded bits output by the encoder as parsing progresses. In particular, as soon as the first block is decrypted, we can extract the message length $|M|$ from the first two bytes which enables us to efficiently resolve possible length ambiguity once parsing is complete.

Assuming that at least one path generates a valid SV, once the entire covertask is parsed we have a set of up to N branches each of which corresponds to a distinct sequence of tokens X_i and a distinct encoding D_i . Having peeked at the length $|M|$ through block-wise decryption of the first block in C , we can shortcut the trial decryption process by truncating any excess symbols from each D_i . If some X_j in this set does indeed match the sequence of tokens produced by decoding the ciphertext record $V||C||T$, then decryption of D_j (or possibly D'_j if $w > 0$) will produce the message M which is returned.

We note that the additional trial decryptions due to parsing ambiguity further reduce the security and correctness guarantees of the AE scheme, although the number of parsing branches is kept small so the impact is minimal.

Optimistic backtracking. It is possible that none of the N parse paths produce a valid decryption, or that all active paths are eliminated before parsing is complete due to parsing failure or SV failure. This will almost certainly happen if the input string is not an authentic covertask produced by our MBFTE system, but it may also happen if our top- N parsing strategy discards the correct path. Using a large N can mitigate the risk of this occurring, but at the cost of generating additional model distributions for each iteration and therefore greatly increasing decode time. For large models like GPT-2, this is the most resource-intensive step of the entire receiver process by far so using a large N can severely degrade overall performance. To mitigate this, we use an optimistic approach with backtracking as follows. We start the process using a small N (e.g., $N = 3$) and if no path produces a valid decryption, we backtrack and restart the process using a larger N . In Section 6, we explore the effects of this approach empirically.

A concrete example. To help make things a bit more concrete, let us offer a simple, back-of-the-envelope analysis. Say that there are $2^{16} = 65536$ non-MBFTE posts that use the same hashtag (overt semantic signal) as the actual MBFTE generated post. Let $N = 8$, i.e., for each of the posts that are scraped by the receiver, there are at most eight partial parsing paths at the time of the SV check. For any particular non-MBFTE post, assume (the worst case) that all eight of the partial parsing paths result in distinct 16-bit patterns where the SV would be. Now, say there are four allowed index values. Since the SVs are 16-bit pseudorandom values, and $4 \ll \sqrt{2^{16}}$ it is overwhelmingly likely that each index value results in a distinct SV. So the number of partial parsing paths that we expect to pass the SV check is roughly $4(8)/2^{16} = 1/2^{11}$. In

other words, for any particular non-MBFTE post, we expect it to be dismissed completely by the SV check, and not to incur the cost of further processing. Across all 2^{16} non-MBFTE posts, we expect about $2^{16}/2^{11} = 32$ to parsing paths *in total* to reach the tag check. Treating HMAC-SHA512 as a good pseudorandom function, any one of the corresponding 32 ciphertext records has roughly a $1/2^{40}$ chance of passing the (40-bit) tag check, so we expect about $32/2^{40} = 1/2^{35}$ to pass. In other words, *only the real MBFTE content* should make it all the way through the receiver-side processing, even when hidden among tens of thousands of other posts.

Covert text length restrictions. If the platform has a post-length restriction, then we may need to fragment our plaintext across multiple covert texts. We describe our approach to fragmentation in Appendix A.1.

5 GPT-2 as MBFTE Model

For our MBFTE-based messaging system we chose OpenAI’s GPT-2 [28] as a generative language model, and in this section, we discuss its relevant characteristics and implementation considerations. Ideally, the language model should be able to produce realistic text in the sense that the resulting covert texts can pass as normal posts on the dead-drop platform. If the covert text stands out from normal platform messages, parties communicating covertly are at risk of being discovered.

GPT-2 is a high-quality language model that has been open-sourced by OpenAI which enables us to fine-tune it for specific content platforms. The fine-tuning process consists of training the model (i.e. tuning its weights) for some additional cycles on a dataset that resembles the output we desire from the model. In our case, this means that we can fine-tune the model on a dataset composed of messages from the dead-drop platform itself, as well as on datasets that include specific semantic signals.

OpenAI has released 4 different versions of GPT-2, which differ in the number of the model parameters (124M, 355M, 774M, and 1.5B). The most realistic text is of course obtained from the version with 1.5B parameters, but this version requires substantially more resources (compute time and memory) than the smaller versions. For our performance and security experiments, we use the smallest (124M) version of GPT-2. By using this version we enable our system to be realistically used on standard off-the-shelf consumer devices, without requiring powerful servers with GPUs.

Parameters, seeds, and token sampling. Like many other language models GPT-2 is *deterministic*, such that with the exact same parameters and seed, the model will always produce the same token distribution. This is a key requirement for MBFTE as it makes our arithmetic coding-based scheme invertible so covert messages can be recovered from a string of tokens. However, this also means that the sender and receiver must share the *exact* same model parameters, including

any subsequent fine-tuning, which sharply limits our ability to adjust model parameters “on the fly” and maintain reliable covert communications. The challenge of synchronizing such shared configuration parameters covertly is an area for future work, and here we assume that the parameters are distributed through the same channels as the system itself.

Given a seed as a context prompt, GPT-2 produces a set of scores called *logits* over the next possible tokens. The larger the logit of a particular token, the more strongly GPT-2 believes this token should be the next one. From logits, there are several ways to choose or sample the next token. A naive approach is to pick the one with the largest logit, but this results in poor quality in practice because the output becomes highly predictable and repetitive. Instead, the logits are meant to be normalized into a probability distribution using the *softmax* function (also called *normalized exponential*).

Concretely, if z_i is the score of the i^{th} token, then the probability of choosing token i is proportional to $\exp(z_i/t)$, where the *temperature* $t > 0$ is a hyperparameter which controls the shape of the distribution. A very low temperature (e.g. 0.1) results in a highly peaked distribution where the largest logit has nearly all of the probability mass, whereas a very high temperature (e.g., 10) results in a nearly uniform distribution over the entire token set. For normal temperature ranges, sampling from the probability distribution directly can sometimes result in very unlikely tokens being selected, which results in awkward-looking output. This is because there will be many tokens in the model’s vocabulary that have small logit scores and therefore low probability, but in aggregate, the probability that one such token is selected may be significant.

To mitigate this problem, there are two widely used sampling methods that restrict the choice of tokens to a subset of the vocabulary. The first is *top- k* sampling, in which only the k most likely tokens are included in the sampling distribution. The second is *top- p* sampling (also called *nucleus sampling* [15]) in which tokens are added to the sampling distribution, in order of decreasing likelihood, until a total probability mass of p has been reached. After restricting the sampling pool with one of these methods, the individual token probabilities are then renormalized to ensure the cumulative probability is 1. As with the model parameters, hyperparameters such as the temperature and sampling strategy must be synchronized between senders and receivers in order to utilize MBFTE successfully.

Finally, as discussed in Section 4, the set of tokens used by GPT-2 is not prefix-free and this can have a significant impact on the efficiency of receiver processing when the covert text string has ambiguous parsings. Given the level of effort required to correctly handle this ambiguity, we were surprised to find that none of the previous work using GPT-2 for model-based steganography [6, 32, 36] addresses it.

Table 1: Performance statistics over 1000 trials. All times reported are measured in seconds.

	Mean (\pm Std)
Capacity per Token	3.81 (\pm 0.36)
Encoded Expansion	10.03 (\pm 1.11)
Plaintext Bits per Covertext Bits	0.08 (\pm 0.01)
Sender-side Time	8.98 (\pm 4.14)
Receiver-side Time All	20.60 (\pm 27.42)
Receiver-side Time (No backtracking)	15.55 (\pm 8.10)
Receiver-side Time (Backtracking)	114.40 (\pm 65.77)
Receiver-side Failure Rate	0.00
Backtracking Rate	0.05

6 Experiments: Performance

In this section, we measure the performance of our proposed system using micro-benchmarks and a concrete platform (i.e., Mastodon).

6.1 Experimental Setup

We use a machine with an Intel Core i7-6700 CPU with 8 GB of RAM. This machine has no dedicated GPU. While our system would run on less powerful machines, we posit that this machine is representative of the average hypothetical desktop user.

The seed for all performance experiments is the line from Isaac Asimov: “*Or maybe it could be put more simply like this: How can the net amount of entropy of the universe be massively decreased?*”. Unless otherwise specified, we use the 124M GPT-2 small model with no fine-tuning. We have experimentally observed that fine-tuning does not significantly impact capacity per token or sender-side/receiver-side processing times.

We select Mastodon as our platform. Mastodon is an open-source decentralized social network that supports micro-blogging features similar to Twitter and Reddit. Mastodon messages are referred to as “toots”. The intended use case of the system reflected in this instantiation is asynchronous message passing where low latency is not a hard requirement.

We stress that MBFTE is a generic construction in the sense that it can accommodate different choices of underlying generative model, platform, or computing devices, all of which yield different tradeoffs in terms of system performance and security.

6.2 Results

Performance metrics. We use top- $k = 100$ sampling with a temperature of 1. We take random alphanumeric strings of varying lengths between 10 to 100 bytes as input messages and measure performance statistics over 1000 trials. Capacity

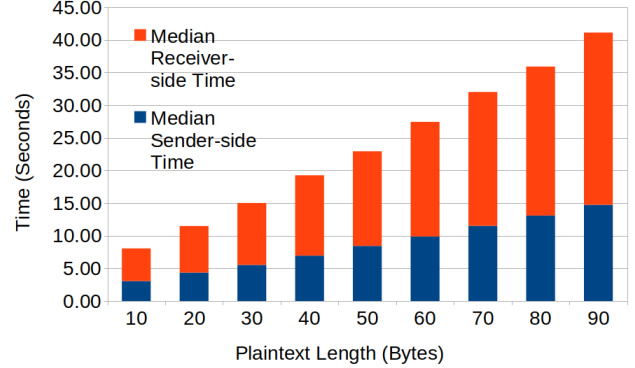


Figure 4: Sender-side processing times and receiver-side processing times for input messages of varying lengths (bytes).

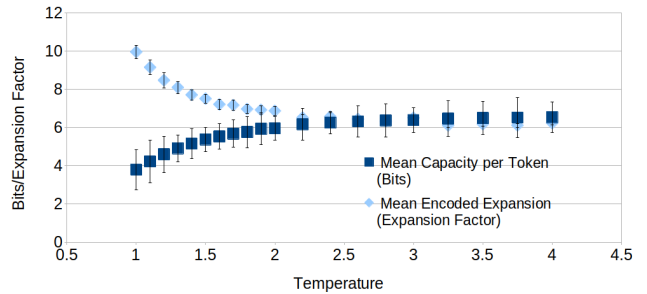


Figure 5: Mean capacity per token and mean encoded expansion versus temperature.

per token is the number of encoded bits (plaintext bits plus record layer bits) divided by the number of generated tokens. Encoded expansion is covertext bits divided by encoded bits. Results are shown in Table 1.

The capacity per token is approximately 3.8 bits, which results in an expansion factor of approximately 10. The average sender-side processing time and receiver-side processing time are approximately 9 seconds and 15.5 seconds, respectively. We also measure the receiver-side processing failure rate. Failure is possible because MBFTE is a probabilistic system and parsing the covertext in terms of the language model’s vocabulary is ambiguous. However, we did not observe any decoding failure in our experiments. We did observe backtracking in about 5% of the cases, which delayed receiver-side processing. We discuss the relationship between backtracking rates and temperature for both top- p and top- k sampling strategies in Appendix B.3.

Sender-side processing and receiver-side processing time per message length. We also measured the sender-side processing and receiver-side processing time for various lengths of input messages (Fig. 4). We binned messages according to their length in bytes in ten bins. The number of samples for each bin ranged from 96 to 131. We observe that although

Table 2: Sample platform messages. Left: regular platform messages scraped from Mastodon #news posts. Right: Sample MBFTE messages (produced using GPT-2 fine-tuned on Mastodon #news posts)

Sample of regular platform messages (Mastodon #news Posts)	Sample MBFTE messages
Sir David Attenborough spent lockdown 'listening to birds'	CNN: Giant lizard dubbed 'Jaws of Death' just made the first record in the world for size, in the largest aquatic lizard ever found
[Post Game Thread] The Miami Heat defeat the Boston Celtics 125-113 behind 32/14/5 from Bam Adebayo to win the series 4-2 and advance to the NBA Finals	BREAKING: The New York Islanders have hired Peter Green, who has spent nearly 20 years as a head coach at the University of Notre Dame, and hired Steve Nash, an assistant football coach for the Islanders, reports USA Today.
First community solar-storage project completed in New York	COVID-19: Child care-deposit boxes inspire movement
Fossilised leaves from Jurassic period found in Jharkhand	TUI: Doctor who lost possession of possession wins battle
Remnants of an ancient asteroid shed new light on the early solar system	'Hi, This Is Spartacus': Creator shares first look at his latest miniseries

the sender-side processing and receiver-side processing times increase with longer plaintext lengths, the increase appears to be linear and the overall times are such that the overall latency to get a message from Alice to Bob is reasonable provided communication is sporadic and messages are not unreasonably long.

Temperature and capacity tradeoff. We measured the capacity per token while varying temperature. This is shown in Fig. 5, where it can be seen that capacity per token increases steadily from below 4 bits per token at temperature 1, to 6 bits per token at temperature 2, whereafter it plateaus as temperature increases. The relationship to encoded expansion is inverted. That is, encoded expansion takes an expansion factor value of 10 at temperature 1, where then it steadily decreases to around 7 at temperature 2, and from there plateaus. It is worth keeping in mind that although higher temperature produces higher capacity, it also lowers the naturalness of the covertext, as shown by increased detectability in Section 8.

Platform times. We used the Python wrapper for the Mastodon API [14] to post and scrape messages and found that the time to post and scrape is essentially just that of the network round-trip time¹. This means that performance is bottlenecked by local operations. On top of the regular receiver-side processing, some of the time spent by the receiver is picking an MBFTE message out of a collection of Mastodon toots because this requires identifying the message (through checking of hashtag and sentinel value).

To quantify this we measure the time for the receiver to pick the MBFTE message out of a collection of 100 messages (99 real Mastodon toots, 1 MBFTE message) when the collection is in random order. Over 50 trials, this process took 32.6 seconds (± 16.8 seconds). This result shows that it is feasible for the receiver to periodically poll the platform in order to retrieve new MBFTE messages. Given that Mastodon, Twitter, and Reddit provide functionality for chronologically viewing posts it is not difficult to check all messages in a given time period, thus allowing for this complete scraping on a target set of posts.

¹It should be noted that the Mastodon API rate limits by IP address to 300 requests per 5 minutes

Sample messages. In Table 2 we show some sample MBFTE messages (with GPT-2 finetuned on Mastodon #news) alongside some actual #news Mastodon posts. The MBFTE samples are generated with a temperature of 1 and top- k with $k = 100$. It is worth noting that a full plaintext message alongside the corresponding record-layer header does not always fit in a single post. So when necessary we use fragmentation as described in Appendix A.1 to embed the plaintext into multiple MBFTE covertexts/posts. The receiver can gather all the posts and process them to recover the entire plaintext.

7 Adversaries and Metrics

We do not provide a formal notion of security. Instead, as is common in this space [5, 32, 35, 36], we evaluate security experimentally.

7.1 Adversarial Model & Strategies

We consider an adversary that passively observes messages on the platform with the goal of identifying MBFTE messages and/or MFBTE users. More precisely, the adversary is given a collection of messages from the platform and tasked to classify each message as an “MBFTE” message or as a “normal” platform message. For this, the adversary may have various levels of background knowledge about the MBFTE system, and success is evaluated by the classification errors made. However, the adversary is not in control of the platform, and banning its usage or taking it down is considered too costly in terms of collateral damage. We also assume that the adversary is unable or unwilling to delete or alter messages. Finally, MBFTE is intended for use on a platform with a significant daily volume of messages, so that any detection method must scale to be a viable strategy.

The adversary’s end goal is to identify MBFTE messages directly, or to flag suspicious messages as potentially MBFTE messages for further analysis (e.g., by humans). In both cases, we model the adversary as a binary classifier. The classification decisions are made based on a threshold, which can be varied based on adversarial objectives between the two

types of errors that the adversary can make: false alarms (i.e., false positives) and missed detections (i.e., false negatives). A *false alarm* occurs when the adversary predicts a normal message as MBFTE, whereas a *missed detection* occurs when the adversary predicts an MBFTE message as normal.

Metrics. To compare adversaries, we use a Receiver Operating Characteristics (ROC) curve (which plots true positive rate versus false positive rate) and we calculate the Area Under Curve (AUC). The AUC can be used to compare adversaries since a larger AUC indicates better classification performance and an AUC of 0.5 corresponds to random guessing.

Strategies. However, if we seek to analyze the detectability of MBFTE messages when deployed on a platform, we need to consider the *base rate*, i.e., the proportion of all platform messages that are MBFTE messages. In this case, the adversary must choose a point in the tradeoff curve between the false alarm and missed detection rates since there is no way to simultaneously minimize both. To reflect this, we consider three different strategies: (1) minimizing false alarms, (2) equalized errors, and (3) maximize detection. We describe these strategies in more detail in Appendix C.1. In each case, the success of the adversary is measured by taking both types of errors into account. Taking both types of errors into account is critical because eliminating one type of error (at the cost of the other) is trivial. For example, if the adversary wants to have no missed detections, it suffices to predict “MBFTE” for every message, but obviously, this is not a viable strategy because it also produces the maximum number of false alarms.

Importance of the base rate. An observation is that the adversary’s performance on a randomly selected message does *not* directly translate to its performance at classifying messages on the platform. This is because the base rate impacts the difficulty of the task and the tradeoff between the two types of errors. The base rate is dependent on the level of activity (e.g., Twitter gets 500 million tweets per day) but also the activity of users exchanging covert messages using the MBFTE system. All else being equal, the lower the base rate, the more difficult it is for the adversary to identify MBFTE messages on the platform. The consequence, which may appear to be counter-intuitive at first, is that the higher the activity of MBFTE on the platform the worse it is for security. However, this can be understood as a manifestation of base rate neglect [3], which we illustrate with an example.

Example. Suppose we deploy the MBFTE system on a platform with a high background activity so that MBFTE messages are effectively hidden in a sea of normal messages. In this case, a realistic base rate may be 0.1% or even 0.01%. Take an adversary who never misses detection (i.e., it never predicts normal for a message that is actually an MBFTE message) but who has a small false positive rate of 2% (i.e., in 2% of the cases a normal message is flagged as being MBFTE).

What is the (posterior) probability that if the adversary flags a message as a potential MBFTE message, the message is in fact an MBFTE message? It depends on the base rate. In particular, if the base rate is 0, then the posterior probability is (of course) also 0 even though the classifier will still flag 2% of all platform messages, which for Twitter would be 10 million messages per day. To further emphasize this point: what is the posterior probability if the base rate is 0.1%? A simple calculation using Bayes’ theorem shows this probability to be 0.0476, which is to say that for every 100 messages flagged as potentially MBFTE, we should only expect 4 or 5 of them to actually be MBFTE messages.

7.2 Adversaries & Background Knowledge

We consider several adversaries based on their assumed background knowledge about the task and the MBFTE system.

Outlier detection. This adversary has access to a large representative collection of normal (i.e., non-MBFTE) platform messages, but not to any MBFTE messages. This models an adversary that has no access to the MBFTE system and consequently must treat the task of distinguishing MBFTE posts from normal platform messages as an *outlier detection* task. For this adversary, we train a one-class SVM on a large set of Mastodon #news posts.

Message likelihood estimator. This adversary has full knowledge of the inner workings of the MBFTE system, but not the seed or the specific fine-tuned version of the GPT-2 model. This adversary attempts to distinguish MBFTE from normal messages on the platform by estimating the likelihood of a message produced by the model underlying MBFTE. Since language models are not perfect (even when fine-tuned), the distribution of output text does not exactly match that of English text produced by humans. For this adversary, we use GLTR [11], which is designed to identify text produced by GPT-2 models.

State-of-The-Art (SoTA) distinguisher. This adversary has access to a large representative collection of both normal messages and MBFTE messages. This captures an adversary that is able to generate MBFTE messages at will, for example by having access to the MBFTE system itself. We distinguish two variants of this adversary depending on whether the exact fine-tuning is known. For this adversary, we use the RoBERTa detector [26] developed by OpenAI specifically to detect GPT-2 text. On the largest GPT-2 model, this detector achieves 96% accuracy [34].

There are two important remarks. The first is that in keeping with the spirit of Kerckhoffs’ principle, the last adversary (the strongest) knows everything about how the MBFTE system works (including the exact fine-tuning). However, it is still interesting to consider the success rate of weaker adversaries. The second remark is that measuring the adversary’s success

rate this way only provides a lower bound on (in)security, as better classifiers may be developed in the future.

8 Experiments: Security

In this section, we experimentally quantify the security of the MBFTE system. We follow the methodology outlined in Section 7. We are interested in: (1) comparing adversaries and identifying the factors that impact detectability, and (2) understanding detectability in terms of false alarms and missed detections if MBFTE were deployed on a large public platform like Twitter.

8.1 Experimental Setup

For the outlier detection adversary, we use Scikit-Learn to train a one-class SVM [31] on a set of 10,000 messages scraped from Mastodon #news. We vectorize words using gensim’s word2vec [12] model, with a vector length of 100. To process each message in the training data, we average the embedding vectors coordinate-wise. To tune hyperparameters, we performed a grid search with cross-validation. The search settled on an RBF kernel and γ set to its default ‘scale’ value. After training, the model is used to provide a confidence score for each test message that belongs to the training data distribution. If the confidence is below a threshold, we predict that the message does not belong to the training data distribution and thus classify it as MBFTE.

For the message likelihood estimation adversary, we use GLTR [11] to compute the likelihood and rank. We compare this rank to a threshold, to classify the message as MBFTE or normal. We use rank instead of likelihood because it provides better experimental results for the adversary, and it is more robust if the adversary does not know the value of some parameters (e.g., temperature). It is important to note that GLTR is not using the GPT-2 model fine-tuned on Mastodon #news but the base GPT-2 124M model.

For the distinguisher adversary, we use OpenAI’s RoBERTa model. We generate 10,000 MBFTE messages using seeds gathered from Mastodon #news, a temperature of 1, and top- p sampling with $p = 0.99$. For the case where the adversary has knowledge of the fine-tuning, we use the fine-tuned model on Mastodon #news. For the case where the adversary does not know the fine-tuning, we use the base GPT-2 124M model. We include these 10,000 MBFTE messages and add 10,000 messages scraped from Mastodon #news to make a complete training set of 20,000 messages. We train the models using the default parameters values, which include a $2e^{-5}$ learning rate and a batch size of 24 and stop when the training accuracy stops increasing (after about 15-20 epochs).

We use top- $p = 0.99$ sampling when the temperature is 1, and top- $k = 100$ elsewhere. The rationale for this is that according to related research [32] top- p sampling for temperature 1 produces more natural covertext. In our experiments

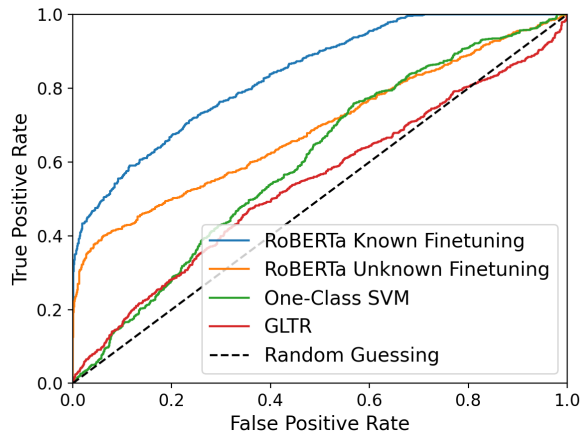


Figure 6: ROC curves for the outlier detection adversary (one-class SVM), message likelihood estimation adversary (GLTR), and SoTA distinguisher adversary (RoBERTa) for fine-tuning known and unknown.

that has been true, $p = 0.99$ is very slightly less detectable compared to $k = 100$, but only when temperature is 1. Otherwise, we have observed negligible differences in their detectability, but with significantly increased decoding time for top- p .

Unless otherwise specified, we use a test set composed of 1,000 MBFTE messages produced by our Mastodon #news fine-tuned GPT-2 124M and 1,000 messages scraped from Mastodon #news. This set is disjoint from the training sets.

8.2 Results

8.2.1 Adversaries’ Classification Performance

We evaluate the classification performance of our adversaries. The corresponding ROC curves are shown in Fig. 6.

The outlier detection (one-class SVM) and message likelihood estimation (GLTR) adversaries are marginally better than random guessing. The respective AUC scores are 0.603 and 0.544. In contrast, the RoBERTa adversaries achieve much higher classification performance. When the exact fine-tuning is known, the AUC is 0.837, whereas it is only 0.687 when the fine-tuning is unknown. This implies that if the adversary does not know the fine-tuning, the detection rate is significantly decreased. Nevertheless, even if the adversary does know the fine-tuning, one should still use the fine-tuning that best represents the platform.

8.2.2 Factors impacting security

Importance of fine-tuning. Our experimental results show that fine-tuning the model used by MBFTE to the target plat-

form produces much more natural text and is critical to reducing the detection of MBFTE posts. We emphasize that this is true regardless of whether the adversary is assumed to have perfect knowledge of the fine-tuning. Indeed, to verify this hypothesis, we use the outlier detection (one-class SVM) adversary trained on normal platform messages to detect MBFTE posts that were produced without any fine-tuning (i.e., with the base GPT-2 small 124M model). We find that the AUC for this task is over 0.954, indicating a very strong detector. In contrast, the same one-class SVM (trained on the exact same training dataset) has an AUC of only 0.603 when trying to distinguish (fine-tuned) MBFTE messages from normal platform messages.

Impact of seeds. Another factor that can mitigate detection is the use of appropriately chosen seeds. The MBFTE construction naturally uses seeds but there are various ways to select seeds and one could always use the empty string as a seed. We use the RoBERTa model trained on fine-tuned MBFTE and evaluate its performance on a test set composed of normal platform messages and MBFTE messages produced without seeds (AUC = 0.923). We then also evaluate its performance on a test set composed of normal platform messages and MBFTE messages produced with seeds taken from normal platform messages (AUC = 0.837).

Impact of temperature. Finally, we consider the impact of temperature on detection. It is appealing to vary the temperature used by MBFTE to meet capacity demands. However, in our experiments, the best case to avoid detection is to use a temperature of 1. We evaluate the performance of the RoBERTa model trained on fine-tuned MBFTE on test sets containing MBFTE messages produced with temperatures 0.7, 1.0, and 3.0. The lowest AUC was obtained for a temperature of 1 (AUC = 0.837), whereas the AUC for temperature 0.7 and 3.0 were AUC = 0.88 and AUC = 0.95, respectively. This disparity is due to the different temperatures and not the different sampling. Temperature 1 performs the best of the tested settings for both top-p and top-k. This suggests that a temperature of 1 is the least detectable setting, which for a fine-tuned model is expected to most faithfully represent the platform [32].

8.2.3 Implications & Discussion

To illustrate the implications of our experimental results, we analyze what would happen if our strongest adversary (RoBERTa model with fine-tuning known) were to monitor the platform messages and attempts to flag potential MBFTE messages. For illustration purposes, we quantify the outcome on a (hypothetical) sample of 10,000 platform messages. We assume that the adversary wants to minimize the false positive rate (FPR = 0.1%), which models an adversary who attempts to minimize false alarms. The results are shown in Table 3. In Appendix C.1, we expand this analysis to take into account

Table 3: Expected outcomes on 10,000 platform messages for the strongest adversary (RoBERTa with known fine-tuning) for varying base rates. The false positive rate is set to 0.1%, which corresponds to a true positive rate of 22.4%. The last row is the posterior probability that a flagged message is in fact an MBFTE message.

	Base rate		
	0.1%	0.01%	0%
Actual MBFTE messages	10	1	0
Total messages flagged	12	10	10
False alarms	10	10	10
Missed detection	8	1	0
MBFTE messages flagged	2	0	0
Posterior probability	0.1832	0.0219	0

alternative strategies in exploring the tradeoff between false alarms and missed detections.

As Table 3 shows, with a base rate of 0.1% only 10 out of the sample of 10,000 messages are actual MBFTE messages and our strongest adversary (FPR = 0.1%, TPR = 22.4%) fails to identify most of the MBFTE messages. The adversary falsely flags 10 normal platform messages in addition to 2 actual MBFTE messages. If the base rate is even lower say 0.01%, then all of the flagged messages are false alarms. In fact, the adversary cannot even distinguish that case from the case where the base rate is 0% (i.e., MBFTE is not used at all). It is also worth noting that while base rates of 0.1% and 0.01% may seem low, they would still allow for 500,000 and 50,000 MBFTE messages to be exchanged per day for Twitter. The takeaway is that for the adversary to mostly flag actual MBFTE messages, the false positive rate needs to be not only very small but significantly smaller than the base rate. However, our results show that in such cases the true positive rate becomes low enough that the vast majority of MBFTE will not be flagged.

The previous analysis applies to the case where the adversary seeks to flag MBFTE messages on the platform. If instead, the adversary suspects a specific user of posting MBFTE messages, then the relevant base rate is the proportion of MBFTE messages that the user has posted, which may be significantly higher thus making easier the task of detection for the adversary. However, for platforms where signing up for new accounts is straightforward, MBFTE users can create multiple accounts and distribute their MBFTE posts among these accounts. In addition, posting non-MBFTE messages from those accounts effectively decreases the base rate. If MBFTE users utilize multiple accounts on the platform, the goal of the adversary is to identify all accounts belonging to the same user. For this, the adversary could use means other than looking at the platform messages (e.g., correlating IP addresses). We leave an in-depth analysis of this to future work.

9 Future Directions

We have considered the most straightforward deployment, where the sender and receiver communicate over a single dead-drop platform. But it is easy to imagine settings in which an additional layer of separation is desired, e.g., sender Alice writes a coartext C_a to one dead-drop platform P_a , but receiver Bob reads from a different platform P_b , and neither wants to know the other's platform. Here a third-party "courier" service would read from P_a and write to P_b . Minimally, the courier would need to know how to translate coartexts formatted for P_a into ones for P_b , preferably *without* needing to recover Alice's plaintext message, and without any direct communication between Alice and Bob (outside of initial setup). This scenario presents fresh challenges. What must Alice and Bob (resp.) share with the courier? How should systems be designed to minimize the workload placed upon the courier, and how might the workload be securely shared among all parties? How do the idiosyncrasies of P_a and P_b interact, and what effect will this have on overall information-carrying capacity, coartext expansion, etc.? If Alice and Bob could communicate (infrequently) over an additional, low-bandwidth channel (say, SMS messages), how might this change the system design landscape?

Our experiments mostly consider untargeted attacks, i.e., settings in which the adversary wants to find suspicious posts on the platform. This is in contrast to targeted attacks, where the adversary suspects (say) Alice of using a platform for covert messaging, and wants to find evidence in support of this. We believe these are two very different attack models, and targeted attacks may require new techniques.

There are other channels that adversaries may attempt to use to detect MBFTE which we have not explored, namely usage pattern analysis. This is because the average user of the platform and an MBFTE user could have different posting frequencies or patterns. To avoid this, models of user activity on the platform could be used to drive MBFTE posting and scraping the platform.

We consider platform posts that consist entirely of natural language text. But other post formats may be of interest: audio and image coartext seem likely, and mixed formats, as well.

Finally, we do not consider how the sender and receiver come to be in possession of a shared key, model parameters, seed, etc. These are important deployment considerations that are often elided and should receive more attention.

References

- [1] Janaka Alawatugoda, Douglas Stebila, and Colin Boyd. Protecting encrypted cookies from compression side-channel attacks. In *International Conference on Financial Cryptography and Data Security*, pages 86–106. Springer, 2015.
- [2] Ross J. Anderson and Fabien A. P. Petitcolas. On the limits of steganography. *IEEE Journal on Selected Areas in Communications*, 14(4), 1998.
- [3] Stefan Axelsson. The base-rate fallacy and the difficulty of intrusion detection. *ACM Transactions on Information and System Security (TISSEC)*, 3(3):186–205, 2000.
- [4] Mihir Bellare, Thomas Ristenpart, Phillip Rogaway, and Till Stegers. Format-preserving encryption. In Michael J. Jacobson, Vincent Rijmen, and Reihaneh Safavi-Naini, editors, *Selected Areas in Cryptography*, pages 295–312, Berlin, Heidelberg, 2009. Springer Berlin Heidelberg.
- [5] Sam Burnett, Nick Feamster, and Santosh S Vempala. Chipping away at censorship firewalls with user-generated content. In *USENIX Security Symposium*, pages 463–468. Washington, DC, 2010.
- [6] Falcon Dai and Zheng Cai. Towards near-imperceptible steganographic text. In *Proceedings of the 57th Annual Meeting of the Association for Computational Linguistics*, pages 4303–4308, 2019.
- [7] Jacob Devlin, Ming-Wei Chang, Kenton Lee, and Kristina Toutanova. Bert: Pre-training of deep bidirectional transformers for language understanding. In *Proceedings of the 2019 Conference of the North American Chapter of the Association for Computational Linguistics: Human Language Technologies, Volume 1 (Long and Short Papers)*, pages 4171–4186, 2019.
- [8] Roger Dingledine, Nick Mathewson, and Paul Syverson. Tor: The second-generation onion router. Technical report, Naval Research Lab Washington DC, 2004.
- [9] Kevin P Dyer, Scott E Coull, Thomas Ristenpart, and Thomas Shrimpton. Protocol misidentification made easy with format-transforming encryption. In *Proceedings of the 2013 ACM SIGSAC conference on Computer & communications security*, pages 61–72, 2013.
- [10] Tina Fang, Martin Jaggi, and Katerina Argyraki. Generating steganographic text with lstms. In *Proceedings of ACL 2017, Student Research Workshop*, pages 100–106, 2017.
- [11] Sebastian Gehrmann, SEAS Harvard, Hendrik Strobelt, and Alexander M Rush. Gltr: Statistical detection and visualization of generated text. *ACL 2019*, page 111, 2019.
- [12] Gensim. Topic modeling for humans. <https://radimrehurek.com/gensim/>.
- [13] Yoel Gluck, Neal Harris, and Angelo Prado. Breach: reviving the crime attack. 2013.

- [14] Halcy. halcy/mastodon.py. <https://github.com/halcy/Mastodon.py>.
- [15] Ari Holtzman, Jan Buys, Li Du, Maxwell Forbes, and Yejin Choi. The curious case of neural text degeneration. In *International Conference on Learning Representations*, 2020.
- [16] Paul G Howard and Jeffrey Scott Vitter. Practical implementations of arithmetic coding. In *Image and text compression*, pages 85–112. Springer, 1992.
- [17] Gabriel Kaptchuk, Tushar M. Jois, Matthew Green, and Aviel Rubin. Meteor: Cryptographically secure steganography for realistic distributions. Cryptology ePrint Archive, Report 2021/686, 2021. To appear in ACM CCS 2021.
- [18] John Kelsey. Compression and information leakage of plaintext. In *International Workshop on Fast Software Encryption*, pages 263–276. Springer, 2002.
- [19] Tri Van Le and Kaoru Kurosawa. Bandwidth optimal steganography secure against adaptive chosen stego-text attacks. In Jan L. Camenisch, Christian S. Collberg, Neil F. Johnson, and Phil Sallee, editors, *Information Hiding*, pages 297–313, Berlin, Heidelberg, 2007. Springer Berlin Heidelberg.
- [20] Maciej Liśkiewicz, Rüdiger Reischuk, and Ulrich Wölfel. Grey-box steganography. In *Proceedings of the 8th Annual Conference on Theory and Applications of Models of Computation*, TAMC’11, pages 390–402, Berlin, Heidelberg, 2011. Springer-Verlag.
- [21] Daniel Luchaup, Kevin P. Dyer, Somesh Jha, Thomas Ristenpart, and Thomas Shrimpton. Libfte: A toolkit for constructing practical, format-abiding encryption schemes. In *23rd USENIX Security Symposium (USENIX Security 14)*, pages 877–891, San Diego, CA, August 2014. USENIX Association.
- [22] Daniel Luchaup, Thomas Shrimpton, Thomas Ristenpart, and Somesh Jha. Formatted encryption beyond regular languages. In *Proceedings of the 2014 ACM SIGSAC Conference on Computer and Communications Security*, CCS ’14, page 1292–1303, New York, NY, USA, 2014. Association for Computing Machinery.
- [23] H Hernan Moraldo. An approach for text steganography based on markov chains. *arXiv preprint arXiv:1409.0915*, 2014. Presented at 41 JAIIO - WSegI 2012.
- [24] Chanathip Namprempre, Phillip Rogaway, and Thomas Shrimpton. Reconsidering generic composition. In Phong Q. Nguyen and Elisabeth Oswald, editors, *Advances in Cryptology – EUROCRYPT 2014*, pages 257–274, Berlin, Heidelberg, 2014. Springer Berlin Heidelberg.
- [25] OpenAI. Better language models and their implications. <https://openai.com/blog/better-language-models/>.
- [26] OpenAI. openai/gpt-2-output-dataset (detector). <https://github.com/openai/gpt-2-output-dataset/tree/master/detector>.
- [27] Liam Porr. My gpt-3 blog got 26 thousand visitors in 2 weeks. <https://liamp.substack.com/p/my-gpt-3-blog-got-26-thousand-visitors>.
- [28] Alec Radford, Jeffrey Wu, Rewon Child, David Luan, Dario Amodei, and Ilya Sutskever. Language models are unsupervised multitask learners. *OpenAI Blog*, 1(8):9, 2019.
- [29] Frank Rubin. Arithmetic stream coding using fixed precision registers. *IEEE Transactions on Information Theory*, 25(6):672–675, 1979.
- [30] Phil Sallee. Model-based steganography. In Ton Kalker, Ingemar Cox, and Yong Man Ro, editors, *Digital Watermarking*, IWDW 2003, pages 154–167, Berlin, Heidelberg, 2004. Springer Berlin Heidelberg.
- [31] Scikit-Learn. One-class svm. <https://scikit-learn.org/stable/modules/generated/sklearn.svm.OneClassSVM.html>.
- [32] Jiaming Shen, Heng Ji, and Jiawei Han. Near-imperceptible neural linguistic steganography via self-adjusting arithmetic coding. In *Proceedings of the 2020 Conference on Empirical Methods in Natural Language Processing (EMNLP)*, pages 303–313, 2020.
- [33] Gustavus J. Simmons. The prisoners’ problem and the subliminal channel. In *Advances in Cryptology: Proceedings of CRYPTO ’83*, pages 51–67. Plenum, 1983.
- [34] Irene Solaiman, Miles Brundage, Jack Clark, Amanda Askell, Ariel Herbert-Voss, Jeff Wu, Alec Radford, Gretchen Krueger, Jong Wook Kim, Sarah Kreps, et al. Release strategies and the social impacts of language models. *arXiv preprint arXiv:1908.09203*, 2019.
- [35] Zhong-Liang Yang, Xiao-Qing Guo, Zi-Ming Chen, Yong-Feng Huang, and Yu-Jin Zhang. Rnn-stega: Linguistic steganography based on recurrent neural networks. *IEEE Transactions on Information Forensics and Security*, 14(5):1280–1295, 2018.

[36] Zachary Ziegler, Yuntian Deng, and Alexander M Rush. Neural linguistic steganography. In *Proceedings of the 2019 Conference on Empirical Methods in Natural Language Processing and the 9th International Joint Conference on Natural Language Processing (EMNLP-IJCNLP)*, pages 1210–1215, 2019.

Table 4: Sender-side processing and receiver-side processing times with a GPU versus a CPU for varying temperature. The second and third columns show the sender-side processing and receiver-side processing times in seconds when using a GPU. The speedup columns shows the ratio of sender-side/receiver-side time with a CPU versus a GPU.

Temp.	Time in Seconds – Mean (\pm Std)		Speedup	
	GPU Sender-side	GPU Receiver-side	Sender	Receiver
1	2.65 (\pm 1.33)	4.85 (\pm 2.45)	3.33	3.80
1.5	1.80 (\pm 0.84)	3.97 (\pm 4.23)	3.12	2.79
2	1.42 (\pm 0.64)	3.21 (\pm 4.46)	3.80	3.78
3	1.26 (\pm 0.53)	3.01 (\pm 3.04)	3.90	3.82
4	1.34 (\pm 0.59)	2.59 (\pm 2.00)	3.64	3.51

A Additional Considerations for The MBFTE System

A.1 Fragmentation

Some dead-drop platforms have a limit on the length of each post so that only messages of L characters or less are supported. This means that if our input plaintext M is too long, we need to fragment it across multiple coverttexts. But this is more difficult than it might seem, because we don’t know *a priori* how to fragment. In particular, we don’t know how many characters will appear in each model sample, until we actually do the sampling. Hence, we don’t know how many plaintext bits we can encode into model samples before hitting the coverttext-length limit.

That said, our use of CTR-mode encryption allows us to “pretend” as if we *do* know where the fragmentation boundaries are. This is because CTR mode allows us to encrypt the plaintext one bit at a time, in an online fashion. Thus we can pause encryption of the input message when our coverttext has reached the coverttext-length limit, insert control information (e.g., the fragment index, number of trailing padding bits in the previous fragment) into the plaintext, and continue on.

Note that when fragmentation is employed, one may want to append a sentinel value to each fragment; in particular, when each fragment will result in a distinct platform post. The effective ciphertext record (which is encoded into model samples) would then be $V_1 || C_1 || V_2 || C_2 || \dots || V_\ell || C_\ell || T$, where each C_i is the CTR-mode encryption of an plaintext fragment, and where the tag T covers everything that precedes it. Note that including a SV for each fragment does come at a cost that grows linearly in the number of fragments. In addition, care should be taken to avoid creating so many fragments that the sender is forced to post a conspicuous number of coverttexts to the platform.

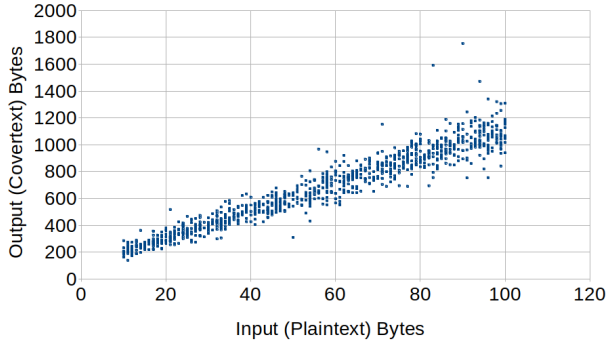


Figure 7: Covertext length (bytes) vs plaintext length (bytes).

B Additional Performance Experiments

B.1 Performance with a GPU

It is well-known that neural networks enjoy a large speedup from running on a GPU (as opposed to a CPU). To quantify this, we use a server equipped with an Intel(R) Xeon(R) Gold 6128 CPU (3.40GHz) with 96 GB of RAM and four Nvidia GeForce RTX 2080 Ti cards, but note that only one GPU is used at a time for the micro-benchmarks. We measure the performance of MBFTE sender and receiver processing using this server on plaintexts of length between 10 and 100 bytes selected uniformly at random.

Table 4 shows the results. When using a GPU, sender-side processing and receiver-side processing take only a few seconds, which results in a speedup of between 3X and 4X in most cases compared to using a CPU. We also see that both sender-side processing and receiver-side processing times are lower for increasing temperature. This is because as temperature increases, the capacity increases which results in fewer tokens being needed to embed the same information and thus less computation.

B.2 Covertext Expansion

We explore the relationship between the length of the covertext in bytes and the length of plaintext (i.e., message) in bytes. Fig. 7 shows a scatter plot of this relationship. It can be seen that the relationship is linear (as expected) but also that there is significant variation in the length of the covertext due to the model’s underlying distribution over the next tokens at each step. Nevertheless, provided that the platform supports posts of a reasonable size (e.g., say 500+ bytes), plaintexts of about 50 bytes will often fit in a single post. For longer plaintexts, fragmentation can be used.

B.3 Backtracking at Higher Temperatures

Recall from Section 4 that we use a Viterbi style top- N decoding procedure where we keep alive the most likely N token

Table 5: Backtracking rate versus Temperature.

Temperature	Backtracking Rate
1	0.03
1.1	0.12
1.2	0.05
1.3	0.07
1.4	0.08
1.5	0.07
1.6	0.12
1.7	0.09
1.8	0.14
1.9	0.15
2	0.13
2.2	0.17
2.4	0.12
2.6	0.16
2.8	0.22
3	0.21
3.25	0.21
3.5	0.15
3.75	0.22
4	0.15

paths. As discussed in Section 6.2, minimizing the number of token paths (N) yields the best performance, but when decoding fails it forces us to backtrack, increase N , and restart the receiver-side process. Specifically, when doing top- k sampling, we use $N = 3$ token paths for optimistic decoding and restart the process with $N = 20$ if this fails. We chose these values because $N = 3$ allows us to decode approximately 95% of messages at low temperature (i.e., temperature of 1 and below), whereas $N = 20$ always results in a success for the remaining 5% of messages. At higher temperatures (i.e., 2 or higher) it becomes more likely that we require more than $N = 3$ paths, so it may be smart to increase optimistic decoding to $N = 4$ or $N = 5$. That being said, top- k sampling gives a hard limit on the number of considered paths, so $N = 3$ is enough for 80% of messages even at temperature 3. However, when using top- p sampling we find experimentally that more tokens are often considered, especially at high temperatures, which results in the need to consider more token paths to properly recover the plaintext. Thus, we use $N = 5$, and increase to $N = 10$ if decoding fails, and finally $N = 30$ if that fails.

We further explore the relationship between backtracking rate and temperature in Table 5. We observe that the temperature is somewhat positively correlated with a high backtracking rate. When backtracking is necessary for decoding, the receiver-side processing time significantly increases.

B.4 Performance at Higher Temperatures with Top- p Sampling

Table 6 shows performance statistics when using top- p sampling instead of top- k sampling. While top- p has a higher capacity than top- k sampling, we only recommend its use when temperature is 1. This is because top- p works by sampling tokens from the probability distribution until their cumulative probability is equal to p . This is ideal for lower temperatures because it allows the distribution to represent all likely tokens, allowing for greater capacity without sacrificing text quality. Unfortunately, this quality is not preserved at higher temperatures. At temperatures 2 and higher the distribution is nearly flat, so sampling tokens up to a specific probability gives a very large number of tokens regardless of their likelihood as a next token. This has no benefits in terms of output text quality. It also greatly increases decoding time, since many paths must be considered when every next token call returns thousands of potential tokens.

C Additional Security Experiments

C.1 Adversarial Strategies

In this section, we discuss and analyze the effect of various adversarial strategies for identifying MBFTE messages.

Strategies Although the adversary cannot control the base rate, they can control the classifier’s threshold which provides a trade-off between false alarms and missed detection. In other words, the adversary can choose a trade-off point on the ROC curve of true positive rate versus false positive rate. To reflect this, we consider three different strategies.

Minimize false alarms: if the adversary wants to be conservative about flagging posts as MBFTE, they may err on the side of minimizing false alarms. For example, this may be setting a very low false positive rate such as 0.1%. The corresponding true positive rate is then determined by the ROC curve.

Equal errors: if the adversary has no preference for minimizing false alarms at the cost of a high rate of missed detection (or vice-versa), then they may elect to choose the point on the trade-off curve where the false positive rate and false negative rate are equal.

Maximize detection: if the adversary wants to avoid missing any MBFTE messages, they should maximize the true positive rate. For example by setting the true positive rate to 90%. The corresponding false positive rate is then determined by the ROC curve. An adversary who engages in this strategy does not care about the cost of falsely flagging many normal messages, which makes sense if (for example) the adversary has the means to and intends to remove all flagged messages from the platform to prevent covert communication.

Implications & Discussion. To understand the security im-

plications for the MBFTE system, we analyze what happens if the strongest adversary (RoBERTa model with fine-tuning known — Section 8.2) monitors the platform messages and flags potential MBFTE messages according to the three previously defined strategies. To illustrate this, we consider a (hypothetical) sample of 10,000 platform messages and vary the base rate (1%, 0.1%, and 0.01%). For each of the three strategies, we use the ROC curve to determine the true positive and false positive rates and then use this to calculate expected outcomes. Results are shown in Table 7. It is seen that (with the possible exception of the case where the false positive rate (FPR) is lower than the base rate) the proportion of messages flagged that are in fact not MBFTE messages is significant and in some cases so large as to make automated detection of MBFTE non-viable for the adversary.

For the minimize false alarms strategy, it may appear that the number of flagged messages is small enough to seek human help. However, for a large public platform like Twitter, even a false positive rate as low as 0.001 means falsely flagging over 500,000 messages per day. Furthermore, if the base rate is equal to or lower than the false positive rate, the proportion of flagged messages that are in fact MBFTE is quite small. In addition, the rate of missed detection that comes as a result of seeking such a low false positive rate means that most MBFTE messages will not be flagged.

For the other two strategies, the number of flagged messages is so large as to make the identification of MBFTE messages completely impractical. However, for the maximize detection strategy, an adversary that has some control over the platform or the individuals that can access it may decide to remove all messages flagged or prevent access to the platform for all users with a flagged message. In this case, however, note that about 10% of MBFTE messages will not have been flagged.

Table 6: Performance with top- p strategy.

Temperature	Receiver-side Fail Rate	Backtracking Rate	Mean (\pm Std)		
			Capacity per Token	Sender-side Time	Receiver-side Time
0.7	0	0	2.56 (\pm 0.78)	7.25 (\pm 5.11)	11.60 (\pm 7.42)
1	0	0.50	5.44 (\pm 1.04)	3.09 (\pm 0.78)	94.82 (\pm 77.94)
2	0.05	0.95	13.90 (\pm 0.77)	2.78 (\pm 0.69)	295.54 (\pm 83.41)
3	0	1	14.96 (\pm 0.32)	3.08 (\pm 0.58)	316.74 (\pm 64.41)

Table 7: Expected outcomes for the three adversarial strategies on 10,000 platform messages for various base rates for the strongest adversary (RoBERTa with known fine-tuning). For each strategy, we show the false positive rate (FPR) and true positive rate (TPR). The last row is the probability that a flagged message is in fact an actual MBFTE message. Note that this is computed using Bayes’ theorem and thus only approximately equal to the ratio of actual MBFTE messages flagged to the total number of messages flagged.

	Minimize False Alarms			Equal Errors			Maximize Detection		
	FPR=0.001, TPR=0.224			FPR = 0.265, TPR=0.734			FPR=0.499, TPR=0.901		
	Base rate			Base rate			Base rate		
	1%	0.1%	0.01%	1%	0.1%	0.01%	1%	0.1%	0.01%
Num. Actual MBFTE Messages	100	10	1	100	10	1	100	10	1
Total Messages Flagged	32	12	10	2697	2655	2651	5030	4994	4990
False Alarms	10	10	10	2624	2648	2650	4940	4985	4989
Missed Detections	78	8	1	27	3	0	10	1	0
Actual MBFTE Messages Flagged	22	2	0	73	7	1	90	9	1
Probability Flagged Message is MBFTE	0.6935	0.1832	0.0219	0.0272	0.0028	0.0003	0.0179	0.0018	0.0002